

Exploring biomarkers for uterine leiomyosarcoma via combination of iMDM algorithm and pathway enrichment analysis

Haiyang Jiang*, Luyun Qu*, Zenghui Li, Xiaohong Li, Jing Wang, Jianqing Hou

Department of Gynecology, The Affiliated Yantai Yuhuangding Hospital of Qingdao University Medical College, Yantai (China)

Summary

Objective: To understand the pathogenesis and etiology of uterine leiomyosarcoma (ULMS) at its early age, as well as explore an effective method for the treatment of it. **Materials and Methods:** First of all, the gene expression profile data of ULMS and the protein-protein interaction (PPI) data were recruited and preprocessed. Then, the inference of multiple differential modules (iMDM) algorithm, which contained differential co-expression network (DCN) construction and identification of multiple differential modules (M-DMs) in DCN was introduced to identify candidate M-DMs. In the following, the M-DMs were identified via statistical analysis was conducted. Finally, Kyoto Encyclopedia of Genes and Genomes (KEGG) pathway enrichment analysis was conducted to disclose the function of these M-DMs. **Results:** A DCN consisting of 1656 nodes (4182 edges) was built, and 16 seed genes were exacted from the DCN by ranking the z-scores in descending order and setting the threshold value of the top 1%. After refinement, 12 candidate M-DMs were obtained and all of these M-DMs resulted to be M-DMs. The pathway enrichment analysis indicated that five modules were enriched in mRNA Splicing pathway, and three modules were enriched in Gene Expression pathway. The authors predicted that these two pathways and the 12 seed genes might play important roles during the process of the occurrence and development of ULMS. **Conclusions:** This method that was used in the present study to perform the analysis on ULMS was suitable. The authors predict that the results could offer investigators valuable resources for better understanding the underlying mechanisms ULMS on the gene level, and the results will give great insights to reveal pathological mechanism underlying this disease, or even provide a hand for future study of related disease research.

Key words: Uterine leiomyosarcoma; Multiple differential modules; Protein-protein interaction network; Pathway; Biomarker.

Introduction

Uterine leiomyosarcoma (ULMS) always originating in the myometrium, is a frequent malignant gynecologic mesenchymal tumor with an overall poor prognosis [1]. It accounts for 30~40% of uterine sarcoma and approximately 1.3% of malignant tumors [2]. Surgery is the primary treatment modality. Although surgical staging and nomograms can help predict clinical outcome, the five-year survival rate for uterus-confined disease remains less than 50% [3]. Most of the patients still suffer from local and distant recurrence after radical surgical treatment [4]. At the same time, the clinical benefit of adjuvant chemotherapy and radiation therapy methods for the recurrent patients is also very limited [5]. Thereby, to explore a new effective method for the treatment of ULMS is necessary.

Over the past years, molecular targeting therapies have shown remarkable achievements against tumours [6]. It had been demonstrated that genes of *OSTN*, *NLGN4X*, *NLGN1*, and so on were overexpressed in primary ULMS [7]. *KLF6SV1* had been found to be a key genes in ULSM from the transgenic mouse model to human disease [8]. Mäkinen *et al.* advocated it for the first time that genes of *TP53*, *ATRX*, and *MED12* were frequently mutated in ULSM [9]. In addition, *Ad-ANS-886* had been indicated to provide a

potentially reliable diagnostic molecular bio-imaging tool to triage patients with suspicious uterine mass [10]. Furthermore, the entire genome sequence was obtained for ULSM [11]. Unfortunately, the exact pathological mechanism of this disease is currently still unclear.

Diseases are always associated with the perturbations of the gene networks. Differential network analysis has been largely applied to functional gene interaction networks [12], protein-DNA interaction networks [13], genetic interaction networks [14], and protein-protein interaction (PPI) networks [15]. The highly connected differentially expressed genes called hub genes are the focus of the entire analysis. However, it occurs frequently that the genes perturbed are connected with the entire gene modules but not on their own. To thoroughly understand the progress of the disease, it is necessary to perform analysis on the coherently differentially expressed gene modules. Fortunately, the inference of multiple differential modules (iMDM) algorithm, which contains differential co-expression network (DCN) construction and identification of multiple differential modules (M-DMs) in DCN, can identify these sets of genes that are not differentially expressed but also exhibit corrected expressed as a module. In this case, the gene modules with differential activities can be captured, which might be

*Co-first authors and equal contributors.

Revised manuscript accepted for publication September 5, 2017

closely associated with the occurrence and development of the disease.

In this research, based on the PPI network, an M-module algorithm was introduced to conduct analysis on the DCN to mine M-DMs that were not only differentially expressed under diseased states but that also exhibit correlated expression pattern in the network, in order to identify prognostic biomarkers for ULMS. The results might provide guidelines for understanding the pathogenesis and etiology of ULMS at its early stage, as well as to explore effective method for the treatment of it in the near future.

Materials and Methods

Prior to analysis, the gene expression profile of ULMS, with accessing number E-GEOD-64763, was obtained from European Molecular Biology Laboratory-European Bioinformatics Institute (EMBL-EBI) database (<https://www.ebi.ac.uk/>). E-GEOD-64763 existed on A-AFFY-33 - Affymetrix GeneChip Human Genome HG-U133A 2.0 [HG-U133A_2] platform, 54 samples (29 normal myometrium and 25 ULMS) were selected to perform our research.

Having obtained all of the data, robust multichip average (RMA) method [16] and quantiles-based algorithm [17] were introduced to eliminate the influence of non-specific hybridization. Then, perfect match and mismatch values were revised by Micro Array Suite 5.0 (MAS 5.0) algorithm [18], and the value was selected through the median method. Finally, the gene expression profile on probe level was converted into gene symbol level, a total of 12,436 gene symbols were obtained for further analysis.

Search Tool for the Retrieval of Interacting Genes/Proteins (STRING, <http://string-db.org/>) is a database of known and predicted protein interactions. In the present study, the global PPI network was integrated from STRING. A total of 787,896 interactions (16,730 genes) of human beings were gained. The interactions of whose relationship value > 0.2 were retained to construct the original PPI network. In addition, a novel new gene expression profile consisted of 10,906 genes were gained by mapping the pre-processed gene expression profile onto the original PPI network, and the gene pairs were taken out to perform the further analysis.

To perform a coherently differentially expressed gene modules analysis on the entire gene modules, a DCN was constructed to perform the further analysis. To achieve this, a binary co-expression network was firstly built. Based on the gene pairs extracted from the novel new gene expression profile, Pearson correlation coefficients (PCC) [19] was implemented to determine the correlation of each gene pairs in disease condition. $|PCC| \geq 0.8$ of the edges was chosen as the cut off value for selecting the genes pairs to construct the binary co-expression network. Then, each edge of the binary co-expression network was assigned a weight value on account of differential gene expression between the disease and the normal control condition. In the present study, EdgeR [20], a Bioconductor package for differential expression analysis of digital gene expression data was utilized to detect differential gene expression for the microarray data. Prior to performing analysis with EdgeR, p -values of differential gene expression between the disease and the normal control condition were determined via one-sided Student's t -test. Then the weight $w_{s,m}$ on edge (s, m) in the differential network was calculated as following:

$$w_{s,m} = \begin{cases} \frac{(\log p_s + \log p_m)^{1/2}}{(2 * \max_{k \in N} \log p_k)^{1/2}}, & \text{if } cor(s,m) \geq \delta, \\ & \text{if } cor(s,m) < \delta, \end{cases}$$

Where p_s and p_m were p -values of differential expression f genes s and m, respectively. N was the node set of the co-expression network, and $cor(s, m)$ was the absolute value of PCC between genes s, m based on their expression profiles. Under this weighting scheme, genes that were co-expressed and significantly differentially expressed were assigned higher weights, which satisfied the present authors' assumption that those genes likely participated in a pathway that exhibited differential activities between the two conditions being compared. Therefore, a DCN for ULMS was built.

To capture the dynamic changes in gene modules under different conditions, M-DMs were mined via the M-module algorithm [21]. M-DMs searching consisted of the following three steps: seed prioritization, module searching by seeds expansion, and refinement of candidate modules.

First of all, the genes contained in the DCNs were ranked based on the degree centrality features of the genes in the network. To be specific, for each network $G_q = (N, E_q)$ ($1 \leq q \leq Q$) with an adjacency matrix A_{\cup} , the importance of the gene u in each DCN was calculated according to the following formula:

$$g(u) = \sum_{v \in N_h(u)} A'_{uv} g(v)$$

Where $g(u)$ denoted the importance of vertex x in the corresponding network; $N_u(v)$ denoted the set of neighbors of v in G_q ; A'_u denoted the degree normalized weighted adjacency matrix. The product $A'-g$ denoted the information propagation on network via the edges of networks, which indicated that the importance of a node depends on the number of its neighbors, strength of connection, and importance of its neighbors.

According to the computational formula given above, the authors obtained the importance of the genes in all individual networks, which we denoted as z-score values. Then, all of the z-score values were ranked in descending order in all individual networks, and the authors obtained the rank for that gene across all networks by averaging the z-scores across all networks. The top 1% genes were treated as seed genes. First of all, each of the seed genes was chosen as a differential module T . Then, commencing from each seed gene u , the network gene v that adjacent to u was added to T to form a module T' . The entropy decrease between these two modules was calculated according to the following formula:

$$\Delta H(T', T) = H(T) - H(T')$$

$\Delta H(T', T) > 0$ indicated that addition of vertex v improved the connectivity of the former M-module T alternatively added genes that adjacent to u to the module T until there was no decrease in the objective function of ΔH . In this case, all of the genes were connected together to form M-DMs.

In the refinement step, the authors kept only those M-DMs of whose sizes ≥ 5 . In addition, the ratio of intersection over union for two sets was measured by Jaccard index, and the two sets were merged into a module while the Jaccard index ≥ 0.5 .

In the present study, the method of random network was selected to conducted statistical analysis of the candidate M-DMs to identify M-DMs. Each random network contained the same number of the edges in DCN, and then module search analyses were performed according to the method mentioned above; 1000 repetitions were performed so as to ensure the validity of the results. In addition, the empirical p -value of each module was evaluated as the probability of the module with smaller score by chance.

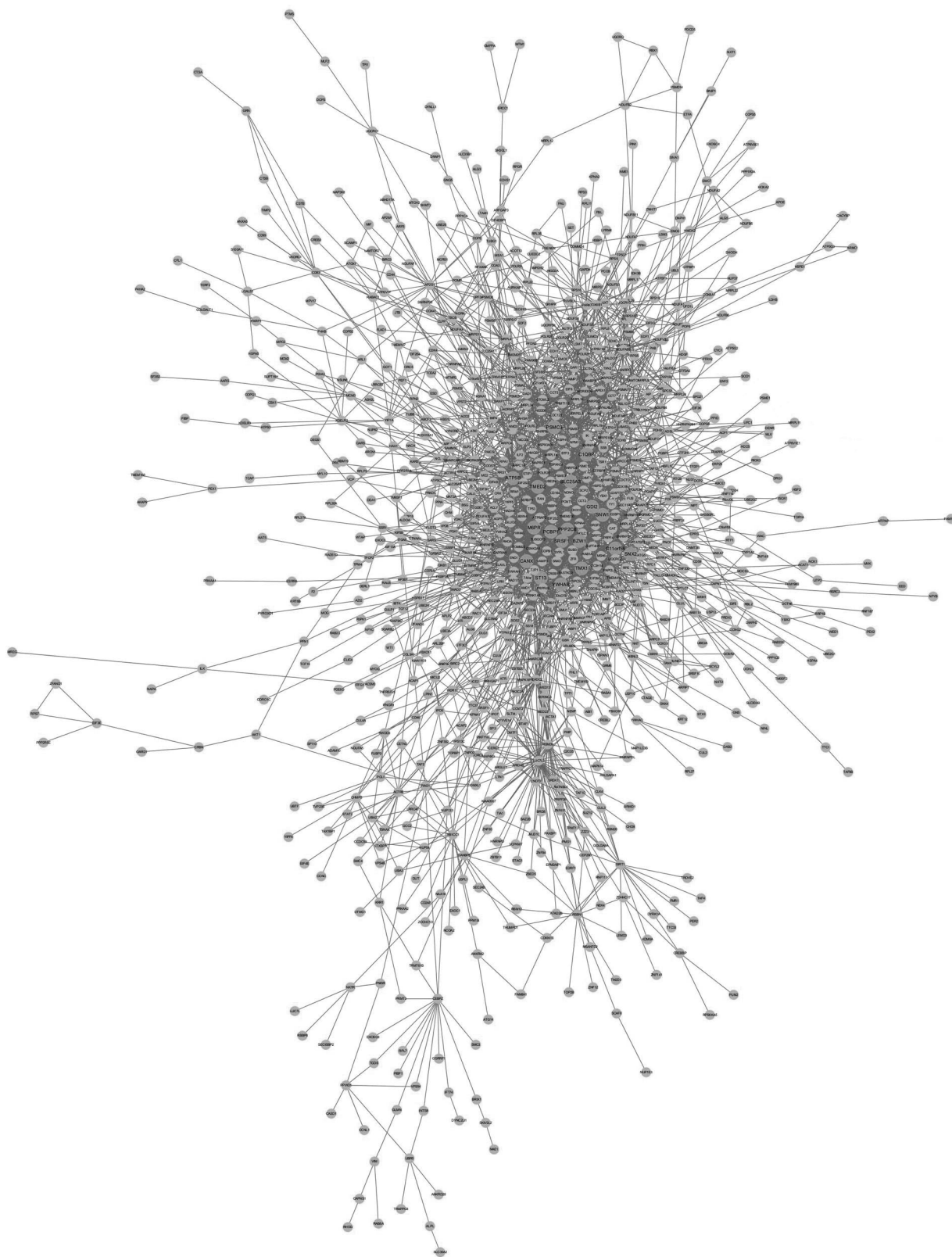


Figure 1. — The main differential co-expression network for uterine leiomyosarcoma constructed based on the absolute value of Pearson correlation coefficients ≥ 0.8 , as well as wiping off these nodes that are not exhibited in close communication with the main network. The orange nodes represent the seed genes.

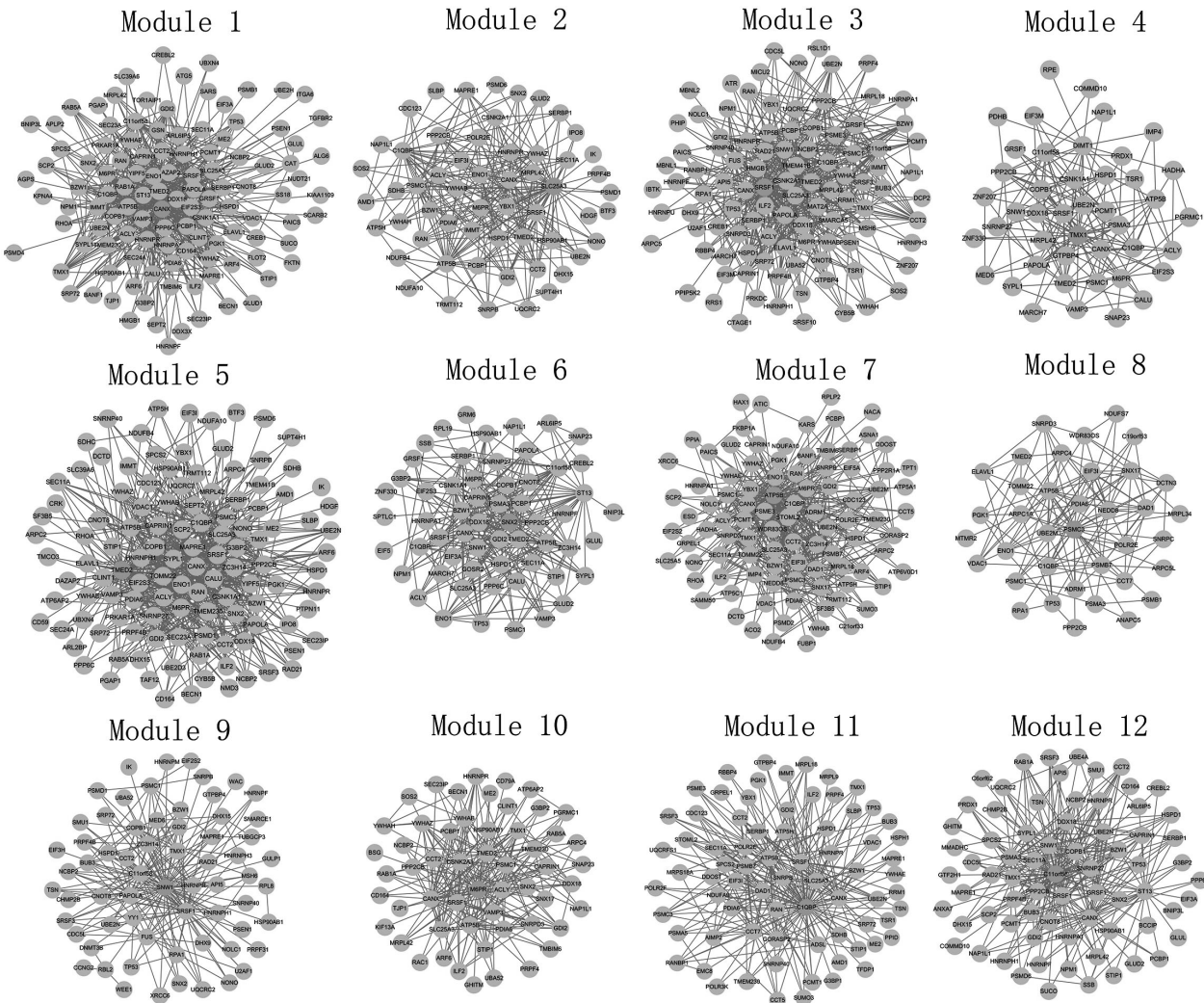


Figure 2. — The 12 multiple differential modules for uterine leiomyosarcoma under the threshold of p -value ≤ 0.05 . The orange nodes represent the seed genes.

The formula was shown as followed:

$$P\text{-value} = \frac{\sum (H_R > H_D)}{H_R}$$

Where H_R stood for the number of modules from randomized networks, H_D was the number of modules from DCN. In addition, the Benjamini-Hochberg [22] method was introduced to adjust the above p -value. Finally, the modules with adjusted p -value ≤ 0.05 were considered to be significant as well as were treated as the M-DMs.

The authors were aware that the difference of the genes between the normal control and the disease condition were manifested via the functions of them. In the present study, pathway enrichment analysis were performed in the Kyoto Encyclopedia of Genes and Genomes (KEGG) database to disclose the function of these M-DMs. The Fisher's exact test [23] was utilized to determine the p -values of the enrichment condition and Benjamini-Hochberg method [24] was performed to conduct multiple testing on the p -values. The cutoff value was set at adjusted p -value < 0.05 , and these pathways with the p -value < 0.05 were considered as the pathways that the certain module enriched in. Moreover, the path-

way that with the minimum adjusted p -value was considered as the significant pathway that the module enriched in.

Results

Having recruited and preprocessed the gene expression profile of ULMS and the PPI data, a PPI network with 10906 genes (575,860 interactions) was built. As PCC was introduced to measure the relationships of these interactions between the normal and disease conditions ($|PCC| \geq 0.8$), a binary co-expression network consisted with 1,656 nodes (4,182 edges) was gained. Then, after the one-sided Student's t -test was introduced to determine the p -values of differential gene expression between the disease and the normal control condition and the EdgeR was utilized to

Table 1. — Details of the differential modules.

| Module | ΔH value | Seed gene | Nodes no. | Edges no. | p -value |
|-----------|------------------|-----------------|-----------|-----------|------------|
| Module 1 | 0.769 | <i>CANX</i> | 114 | 539 | 0.00050 |
| Module 2 | 0.815 | <i>SLC25A3</i> | 57 | 246 | 0 |
| Module 3 | 0.841 | <i>SRSF1</i> | 100 | 497 | 0 |
| Module 4 | 0.738 | <i>TMX1</i> | 44 | 173 | 0.0028 |
| Module 5 | 0.827 | <i>TMED2</i> | 118 | 594 | 0 |
| Module 6 | 0.779 | <i>SNX2</i> | 59 | 285 | 0.00022 |
| Module 7 | 0.811 | <i>ATP5B</i> | 95 | 439 | 0 |
| Module 8 | 0.699 | <i>PSMC3</i> | 37 | 144 | 0.013 |
| Module 9 | 0.772 | <i>SNW1</i> | 65 | 210 | 0.00041 |
| Module 10 | 0.830 | <i>M6PR</i> | 55 | 231 | 0 |
| Module 11 | 0.767 | <i>C1QBP</i> | 74 | 276 | 0.00068 |
| Module 12 | 0.839 | <i>C11orf58</i> | 72 | 278 | 0 |

weight the edges, a DCN with each edge was assigned a weight value was constructed. However, there were some nodes that were not exhibited close communication with the main network, hence the authors wiped off them and only kept the main DCN (Figure 1). We could see that all of the 16 seed genes were contained in the main DCN.

To identify the DMs in the DCN, first of all, the seed genes were identified according to the z -scores of the genes. All of the genes were ranked according to the z -scores in descending order. As the authors set the cut off value of the top 1% z -scores, 16 genes were selected as the seed genes. Each seed genes were chosen as an original differential module to perform module searching analysis and 16 original M-DMs were gained. Furthermore, under the threshold

value of nodes > 5 as well as Jaccard index ≥ 0.5 , 12 candidate M-DMs, which were named Module 1 ~ Module 12 were obtained for further analysis.

Further to determine the significance of these candidate M-DMs, the randomization test was performed on these candidate M-DMs to identify M-DMs. Under the threshold value of $p < 0.05$, the authors found that the p values all of the 12 candidate M-DMs were less than 0.05, which meant that all of the candidate M-DMs were M-DMs (Figure 2). The details of these M-DMs are listed in Table 1. The authors found from the table that all of the p values were small enough, or even close to zero, which meant that the statistical results were effective. In addition, the seed genes of Module 1 ~ Module 12 were as following: *CANX*, *SLC25A3*, *SRSF1*, *TMX1*, *TMED2*, *SNX2*, *ATP5B*, *PSMC3*, *SNW1*, *M6PR*, *C1QBP*, and *C11orf58*.

The 12 M-DMs were separately chosen to perform pathway enrichment analysis according to the method mentioned above. As each result of the pathway analysis was ranked in descending order, and the pathway that with the minimum adjusted p -value, as well as satisfy the cutoff value $p < 0.05$ was considered to be the significant pathway that the M-DM enriched in. The details of the pathway that these 12 M-DMs enriched in are listed in Table 2. The authors could found from Table 2 that Module 1, Module 3, Module 5, Module 9, and Module 12 were enriched in mRNA Splicing pathway, and Module 2, Module 6, and Module 11 were enriched in Gene Expression pathway. The authors predicted that these two pathways might play im-

Table 2. — The KEGG pathway enrichment analysis results of the modules.

| Module | Pathway | p -value | Genes |
|-----------|---|------------------------|--|
| Module 1 | mRNA splicing | 0.0042 | <i>HNRNPA1</i> , <i>HNRNPF</i> , <i>HNRNPH1</i> , <i>HNRNPR</i> , <i>NCBP2</i> , <i>NUDT21</i> , <i>PAPOLA</i> , <i>PCBP1</i> , <i>SRSF1</i> |
| Module 2 | Gene expression | 0.0016 | <i>EIF3I</i> , <i>HNRNPR</i> , <i>IPO8</i> , <i>PCBP1</i> , <i>POLR2E</i> , <i>PSMC1</i> , <i>PSMD1</i> , <i>PSMD6</i> , <i>RAN</i> , <i>SEC11A</i> , <i>SLBP</i> , <i>SNRPB</i> , <i>SRSF1</i> , <i>YWHAB</i> , <i>YWHAH</i> , <i>YWHAZ</i> , <i>YBX1</i> , <i>SUPT4H1</i> |
| Module 3 | mRNA splicing | 4.45×10^{-16} | <i>CDC5L</i> , <i>DHX9</i> , <i>FUS</i> , <i>HNRNPA1</i> , <i>HNRNPF</i> , <i>HNRNPH1</i> , <i>HNRNPR</i> , <i>HNRNPU</i> , <i>NCBP2</i> , <i>PAPOLA</i> , <i>PCBP1</i> , <i>PRPF4</i> , <i>SNRNP40</i> , <i>SNRPD3</i> , <i>SRSF1</i> , <i>SRSF3</i> , <i>YBX1</i> , <i>U2AF1</i> |
| Module 4 | AMER1 mutants destabilize the destruction complex | 0.022 | <i>CSNK1A1</i> , <i>PPP2CB</i> |
| Module 5 | mRNA splicing | 5.07×10^{-6} | <i>HNRNPH1</i> , <i>HNRNPR</i> , <i>NCBP2</i> , <i>PAPOLA</i> , <i>PCBP1</i> , <i>SF3B5</i> , <i>SNRNP40</i> , <i>SNRPB</i> , <i>SRSF1</i> , <i>SRSF3</i> , <i>YBX1</i> |
| Module 6 | Gene expression | 0.0058 | <i>CNOT8</i> , <i>EIF2S3</i> , <i>EIF3A</i> , <i>HNRNPA1</i> , <i>HNRNPF</i> , <i>PAPOLA</i> , <i>PCBP1</i> , <i>PSMA3</i> , <i>PSMC1</i> , <i>SEC11A</i> , <i>SNW1</i> , <i>SRSF1</i> , <i>EIF5</i> , <i>SSB</i> , <i>TP53</i> , <i>RPL19</i> |
| Module 7 | Mitochondrial protein import | 6.27×10^{-6} | <i>ACO2</i> , <i>ATP5A1</i> , <i>ATP5B</i> , <i>GRPEL1</i> , <i>HSPD1</i> , <i>SAMM50</i> , <i>TOMM22</i> , <i>VDAC1</i> |
| Module 8 | Autodegradation of Cdh1 by Cdh1:APC/C | 5.21×10^{-6} | <i>ANAPC5</i> , <i>PSMA3</i> , <i>PSMB1</i> , <i>PSMB7</i> , <i>PSMC1</i> , <i>PSMC3</i> |
| Module 9 | mRNA splicing | 4.13×10^{-13} | <i>CDC5L</i> , <i>DHX9</i> , <i>FUS</i> , <i>HNRNPF</i> , <i>HNRNPH1</i> , <i>HNRNPM</i> , <i>HNRNPR</i> , <i>NCBP2</i> , <i>PAPOLA</i> , <i>SNRNP40</i> , <i>SNRPB</i> , <i>SRSF1</i> , <i>SRSF3</i> , <i>U2AF1</i> |
| Module 10 | Membrane trafficking | 5.68×10^{-6} | <i>CLINT1</i> , <i>M6PR</i> , <i>SNAP23</i> , <i>SNX2</i> , <i>UBA52</i> , <i>YWHAB</i> , <i>YWHAH</i> , <i>YWHAZ</i> , <i>TJPI</i> , <i>RAC1</i> |
| Module 11 | Gene expression | 9.28×10^{-8} | <i>AIMP2</i> , <i>DDOST</i> , <i>EIF3I</i> , <i>HNRNPR</i> , <i>POLR2E</i> , <i>PRPF4</i> , <i>PSMA5</i> , <i>PSMB7</i> , <i>PSME3</i> , <i>RAN</i> , <i>RBBP4</i> , <i>SEC11A</i> , <i>SLBP</i> , <i>SNRNP40</i> , <i>SRP72</i> , <i>SRSF1</i> , <i>SNRPB</i> , <i>PSMC3</i> , <i>YBX1</i> , <i>YWHAZ</i> , <i>POLR2F</i> , <i>POLR3K</i> , <i>SPCS2</i> , <i>SRSF3</i> , <i>TFDP1</i> , <i>TP53</i> , <i>TSN</i> |
| Module 12 | mRNA splicing | 2.45×10^{-6} | <i>CDC5L</i> , <i>HNRNPA1</i> , <i>HNRNPF</i> , <i>HNRNPH1</i> , <i>HNRNPR</i> , <i>NCBP2</i> , <i>PCBP1</i> , <i>SRSF1</i> , <i>SRSF3</i> |

portant roles during the process of the occurrence and development of ULMS.

Discussion

ULMS is one of the most common neoplasms in the female genital tract, and is relatively rare mesenchymal tumor. According to the data, surgical intervention is virtually the only means of treatment to improve the prognosis of this disease. However, the effect is not desired enough and little is known regarding the biology of ULMS [25]. The mainly reason is that ULMS is resistant to chemotherapy and radiotherapy, and the surgical intervention is virtually the only means of treatment [26]. In this case, it is critical to understand the biology of ULMS, in order to take steps to prevent the initial development of it at its early age.

In the present study, further to understand the exact pathological mechanism of this disease, the authors performed a comprehensive analysis on ULMS based on combining *i*MDM algorithm and KEGG pathway enrichment analysis to reveal the key pathway between the normal control and the disease condition. Finally, 12 M-DMs which begin from 12 seed genes were identified, and 5 M-DMs were enriched in mRNA Splicing pathway, and 3 M-DMs were enriched in Gene Expression pathway. The authors predicted that these two pathways might play important roles during the process of the occurrence and development of ULMS. To uncover the relationships of ULMS between these pathways and seed genes, further discussion was conducted in the following.

As mentioned above, an important reason for the ULMS remains a rare aggressive cancer is that little knowledge regarding the molecular events undergone by ULMS cells in the process of metastasis has not yet been clearly understood. Over the past years, some researchers have attempted their best to clarify molecular events related to ULMS metastasis. Davidson *et al.* indicated that 203 unique probes that were significantly differentially expressed in the two tumor groups based, comparing the global gene expression patterns of primary ULMS and leiomyosarcoma metastases [27]. Genes of *OSTN*, *NLGN4X*, *NLGN1*, *SLITRK4*, *MASP1*, *XRN2*, *ASS1*, *RORB*, *HRASLS*, and *TSPAN7* had proved to be overexpressed in primary ULMS. Another study pointed out that differentially expressed genes between ULMS and normal myometrial samples identified overrepresentation of cell cycle regulation, DNA repair, and genomic integrity [28]. According to the experimental results, the proteasome subunit beta 9 (PSMB9)/ β 1i-deficient mice successfully survived for 12 months of age with a ratio of 37% [29]. Therefore, the gene expression abnormality has been largely accepted to be associated with ULMS although its exact molecular mechanism has not been disclosed. Combining the existing research results with the present ones, the authors predicted that the mRNA Splicing pathway and

Gene Expression pathway played important roles in the process of the occurrence and development of the disease. In the next study, these pathways and genes of *CANX*, *SLC25A3*, *SRSF1*, *TMX1*, *TMED2*, *SNX2*, *ATP5B*, *PSMC3*, *SNW1*, *M6PR*, *C1QBP*, and *C11orf58* could be chosen as biomarkers to perform overall thorough research on ULMS. However, there were still some weaknesses in the present study that must be taken into account. First of all, the microarray data on which the authors performed analysis were downloaded from the existed database instead of obtaining themselves. Secondly, the results of the bioinformatics methods were not verified via experimental verification analysis, and the exact conclusion could only be determined after experimental verification analysis on the results, which the authors will perform next. Although disadvantages existed, the authors believed that this method and the results offered investigators valuable resources for better understanding the underlying mechanisms ULMS on the gene level, and the results will give great insight to reveal pathological mechanism underlying this disease, or even provide assistance in the future study of related disease research.

References

- [1] Schwameis R., Grimm C., Petru E., Natter C., Staudigl C., Lamm W., *et al.*: "The Prognostic Value of C-Reactive Protein Serum Levels in Patients with Uterine Leiomyosarcoma". *PLoS One*, 2014, 10, e0133838.
- [2] Zivanovic O., Jacks L.M., Iasonos A., Jr M.M.L., Soslow R.A., Veras E., *et al.*: "A Nomogram to Predict Postresection 5-Year Overall Survival for Patients With Uterine Leiomyosarcoma". *Cancer*, 2012, 118, 660.
- [3] Hensley M.L., Wathen J.K., Maki R.G., Araujo D.M., Sutton G., Priebat D.A., *et al.*: "Adjuvant therapy for high-grade, uterus-limited leiomyosarcoma: Results of a phase 2 trial (SARC 005)". *Cancer*, 2013, 119, 1555.
- [4] Hoang H.L., Ensor K., Rosen G., Leon P.H., Raccuia J.S.: "Prognostic factors and survival in patients treated surgically for recurrent metastatic uterine leiomyosarcoma". *Int. J. Surg. Oncol.*, 2014, 2014, (919323).
- [5] Yen M.S., Chen J.R., Wang P.H., Wen K.C., Chen Y.J., Ng H.T.: "Uterine sarcoma part III-Targeted therapy: The Taiwan Association of Gynecology (TAG) systematic review". *Taiwanese. J. Obstet. Gynecol.*, 2016, 55, 625.
- [6] Amant F., Lorusso D., Mustea A., Duffaud F., Pautier P.: "Management Strategies in Advanced Uterine Leiomyosarcoma: Focus on Trabectedin". *Sarcoma*, 2015, 2015, 1.
- [7] Davidson B., Abeler V.M., Førsund M., Holth A., Yang Y., Kobayashi Y., *et al.*: "Gene expression signatures of primary and metastatic uterine leiomyosarcoma". *Hum. Pathol.*, 2013, 45, 691.
- [8] Difeo A., Sennet R., Huang F., Levine D., Kalir T., Rijn M.V.D., *et al.*: "KLF6SV1 is a novel uterine leiomyosarcoma gene: From transgenic mouse model to human disease". *Gynecol. Oncol.*, 2011, 120, S8.
- [9] Mäkinen N., Aavikko M., Heikkinen T., Taipale M., Taipale J., Koivistokorander R., *et al.*: "Exome Sequencing of Uterine Leiomyosarcomas Identifies Frequent Mutations in TP53, ATRX, and MED12". *PLoS. Genet.*, 2016, 12, e1005850.
- [10] Khater M.K., Shalaby S.M., Al-Hendy A.A.: "A highly specific molecular bioimaging approach for diagnosis of human uterine leiomyosarcoma". *Reprod. Sci.*, 2016, 23, 262A.

- [11] Barlin J.N., Zhou Q.C., Leitao M.M., Bisogna M., Olvera N., Shih K.K., *et al.*: "Molecular Subtypes of Uterine Leiomyosarcoma and Correlation with Clinical Outcome 1 2". *Neoplasia*, 2015, 17, 183.
- [12] Zhang B., Tian Y., Jin L., Li H., Shih I.M., Madhavan S., *et al.*: "DDN: a caBIG® analytical tool for differential network analysis". *Bioinformatics*, 2011, 27, 1036.
- [13] Luscombe N.M., Babu M.M., Yu H., Snyder M., Teichmann S.A., Gerstein M.: "Genomic analysis of regulatory network dynamics reveals large topological changes". *Nature*, 2004, 431, 308.
- [14] Guénolé A., Srivas R., Vreeken K., Wang Z.Z., Wang S., Krogan N.J., *et al.*: "Dissection of DNA Damage Responses Using Multi-conditional Genetic Interaction Maps". *Mol. Cell.*, 2013, 49, 346.
- [15] Ellis J.D., Barrios-Rodiles M., Colak R., Irimia M., Kim T., Calarco J.A., *et al.*: "Tissue-specific alternative splicing remodels protein-protein interaction networks". *Mol. Cell.*, 2012, 46, 884.
- [16] Ma L., Robinson L.N., Towle H.C.: "ChREBP• Mlx Is the Principal Mediator of Glucose-induced Gene Expression in the Liver". *J. Biol. Chem.*, 2006, 281, 28721.
- [17] Rifai N., Ridker P.M.: "Proposed cardiovascular risk assessment algorithm using high-sensitivity C-reactive protein and lipid screening". *Clin. Chem.*, 2001, 47, 28.
- [18] Pepper S.D., Saunders E.K., Edwards L.E., Wilson C.L., Miller C.J.: "The utility of MAS5 expression summary and detection call algorithms". *BMC Bioinformatics*, 2007, 8, 273.
- [19] Benesty J., Chen J., Huang Y., Cohen I.: "Pearson correlation coefficient". In: Cohen I., Huang Y., Chen J., Benesty J. (eds). *Noise reduction in speech processing*. Heidelberg: Springer, 2009, 1.
- [20] Robinson M.D., McCarthy D.J., Smyth G.K.: "edgeR: a Bioconductor package for differential expression analysis of digital gene expression data". *Bioinformatics*, 2010, 26, 139.
- [21] Ma X., Gao L., Tan K.: "Modeling disease progression using dynamics of pathway connectivity". *Bioinformatics*, 2014, 30, 2343.
- [22] Benjamini Y., Hochberg Y.: "Controlling the false discovery rate: a practical and powerful approach to multiple testing". *J. R. Stat. Soc. Series. B. Stat. Methodol.*, 1995, 57, 289.
- [23] Routledge R.: "Fisher's exact test". In: *Encyclopedia of Biostatistics*. Wiley Online Library: John Wiley & Sons, Ltd., 2005
- [24] Haynes W.: "Benjamini-Hochberg Method". In: *Encyclopedia of Systems Biology*. Dordrecht, The Netherlands: Springer: 2013, 78.
- [25] Hayashi T., Kawano M., Ichimura T., Ida K., Ando H., Zharhary D., *et al.*: "Molecular Pathology and Novel Clinical Therapy for Uterine Leiomyosarcoma". *Ant. Res.*, 2016, 36, 4997.
- [26] Wu T.I., Chang T.C., Hsueh S., Hsu K.H., Chou H.H., Huang H.J., *et al.*: "Prognostic factors and impact of adjuvant chemotherapy for uterine leiomyosarcoma". *Gynecol. Oncol.*, 2006, 100, 166.
- [27] Davidson B., Abeler V.M., Førsund M., Holth A., Yang Y., Kobayashi Y., *et al.*: "Gene expression signatures of primary and metastatic uterine leiomyosarcoma". *Hum. Pathol.*, 2014, 45, 691.
- [28] Barlin J.N., Zhou Q.C., Leitao M.M., Bisogna M., Olvera N., Shih K.K., *et al.*: "Molecular subtypes of uterine leiomyosarcoma and correlation with clinical outcome". *Neoplasia*, 2015, 17, 183.
- [29] Hayashi T., Faustman D.L.: "Development of spontaneous uterine tumors in low molecular mass polypeptide-2 knockout mice". *Can. Res.*, 2002, 62, 24.

Corresponding Author:
 JIANQING HOU, M.D.
 Department of Gynecology
 The Affiliated Yantai Yuhuangding Hospital of
 Qingdao University Medical College
 No. 20 Yuhuangdingdong Road
 Yantai 264000, Shandong Province (China)
 e-mail: houjianqingyt@163.com